nature cell biology

DOI: 10.1038/ncb2019

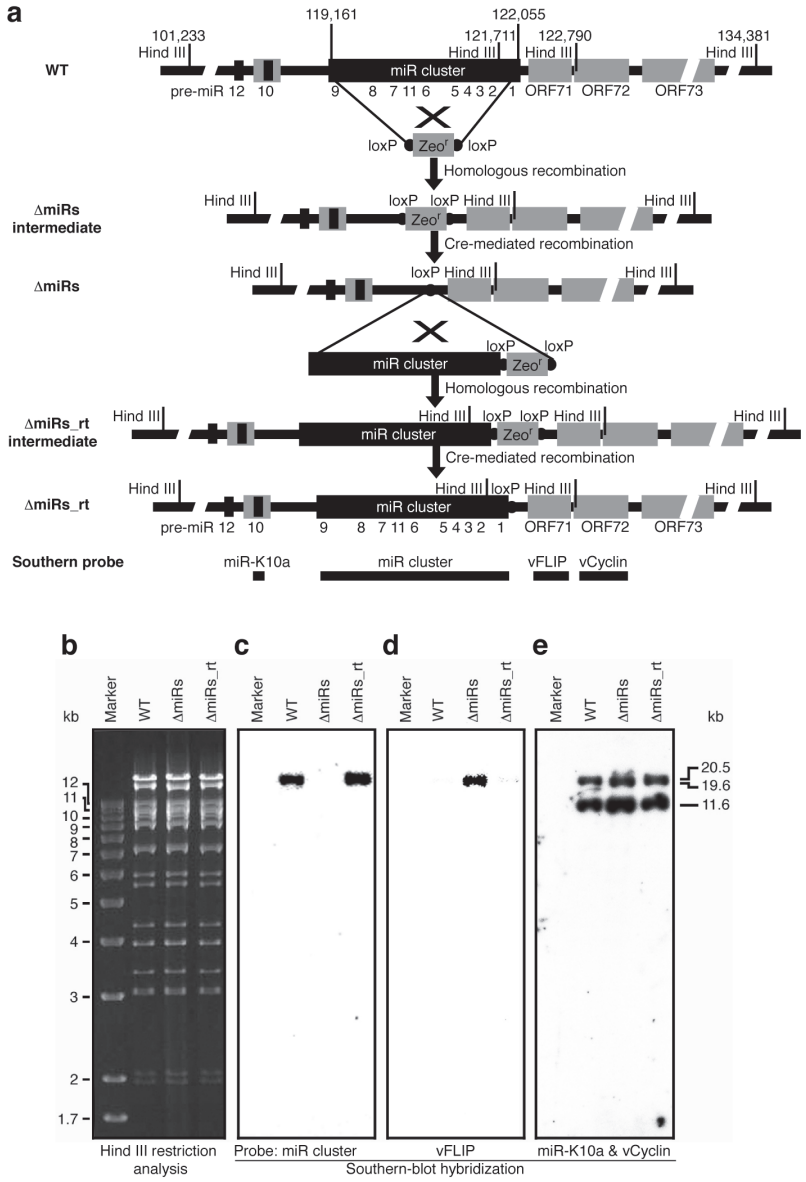

Figure S1 Generation of a KSHV mutant with a cluster of 14 miRs deleted (ΔmiRs) and its revertant (ΔmiRs_rt) using wild-type virus BAC36 (WT). (**a**) Strategy for generating KSHV mutant ΔmiRs and revertant ΔmiRs_rt. Details are described in the Methods. (**b-e**) Genetic analysis of WT, ΔmiRs and ΔmiRs_rt recombinant viruses demonstrating the deletion of the miR cluster in the ΔmiRs genome, which is repaired in the ΔmiRs_rt genome without affecting other parts of KSHV genome. Hind III restriction analysis of WT, ΔmiRs and ΔmiRs_rt genomes (**b**) and Southern-blot hybridization with probe of the miR cluster (**c**), vFLIP (**d**), or combination of miR-K10a and vCyclin (**e**). HindIII digestion showed that WT, ΔmiRs and ΔmiRs_rt recombinant viruses had similar restriction patterns (**b**). WT had three bands in the latent locus including a 20.5 kb band containing all the 17 miRs except miR-K1, a 1.1 kb band containing vFLIP beyond the resolution of the gel, and a 11.6 kb band containing vCyclin and LANA. Deletion of the miR cluster eliminated one HindIII site at position 121,711 generating a new 19.6 kb band derived from the merge of the remaining portions of the 20.5 and 1.1 kb bands. The revertant was identical to WT except the insertion of a LoxP site immediately outside the miR cluster. Southern-hybridization with the miR cluster as a probe detected the 20.5 kb band in the WT and ΔmiRs_rt lanes but not in the ΔmiRs lane (**c**). The vFLIP probe only detected the 19.6 kb band in the ΔmiRs lane but not in the WT and ΔmiRs_rt lanes (**d**). The vCyclin probe detected the 11.6 kb band in all the recombinant viruses while the miR-K10a probe detected the 20.5 kb band in the WT and ΔmiRs_rt lanes but the 19.6 kb band in the ΔmiRs lane (**e**).

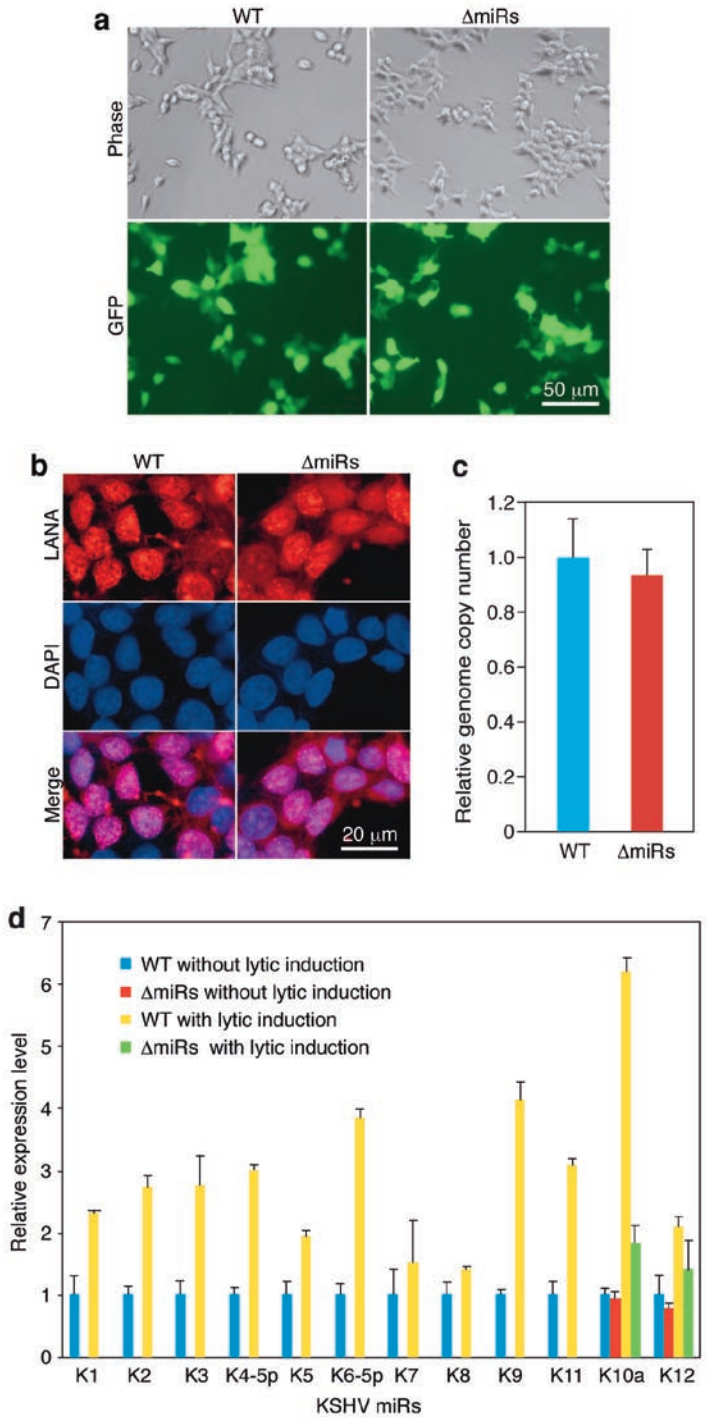

Figure S2 Reconstitution of KSHV recombinant viruses in 293T cells. (**a**) Morphology of WT and ΔmiRs in 293T cells. (**b**) Immunofluorescence staining of LANA with a specific monoclonal antibody showing that all WT and ΔmiRs cells were LANA-positive with similar nuclear staining pattern. (**c**) Relative KSHV genome copy number in WT and ΔmiRs 293T cells determined by quantitative real-time PCR. (**d**) Detection of individual KSHV miRs in WT and ΔmiRs 293T cells. The presence and expression levels of individual KSHV miRs was examined in uninduced WT and ΔmiRs cells, and cells induced with TPA and sodium butyrate for 48 h by quantitative real-time reverse transcription PCR. Data are means ± SEM from three (n = 3) independent experiments (**c, d**). For image panels, representative images from three (**a, b**) independent experiments are presented.

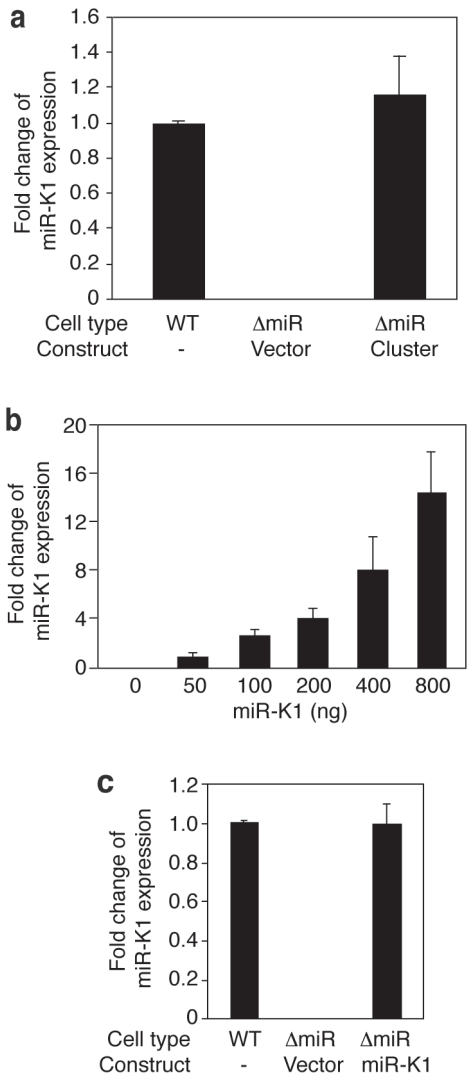

Figure S3 miR-K1 expression detected by quantitative real-time reverse transcription PCR. (**a**) Stable expression of the miR cluster in ΔmiRs cells resulted in the expression of miR-K1 at a level similar to that of WT cells. (**b**) The expression level of miR-K1 increased at a dose-dependent fashion with increasing input of miR-K1 construct DNA in transient transfection in 293T cells. (**c**) Stable expression of miR-K1 in ΔmiRs cells resulted in the expression of miR-K1 at a level similar to that of WT cells. Data are means ± SEM from three (n = 3) independent experiments.

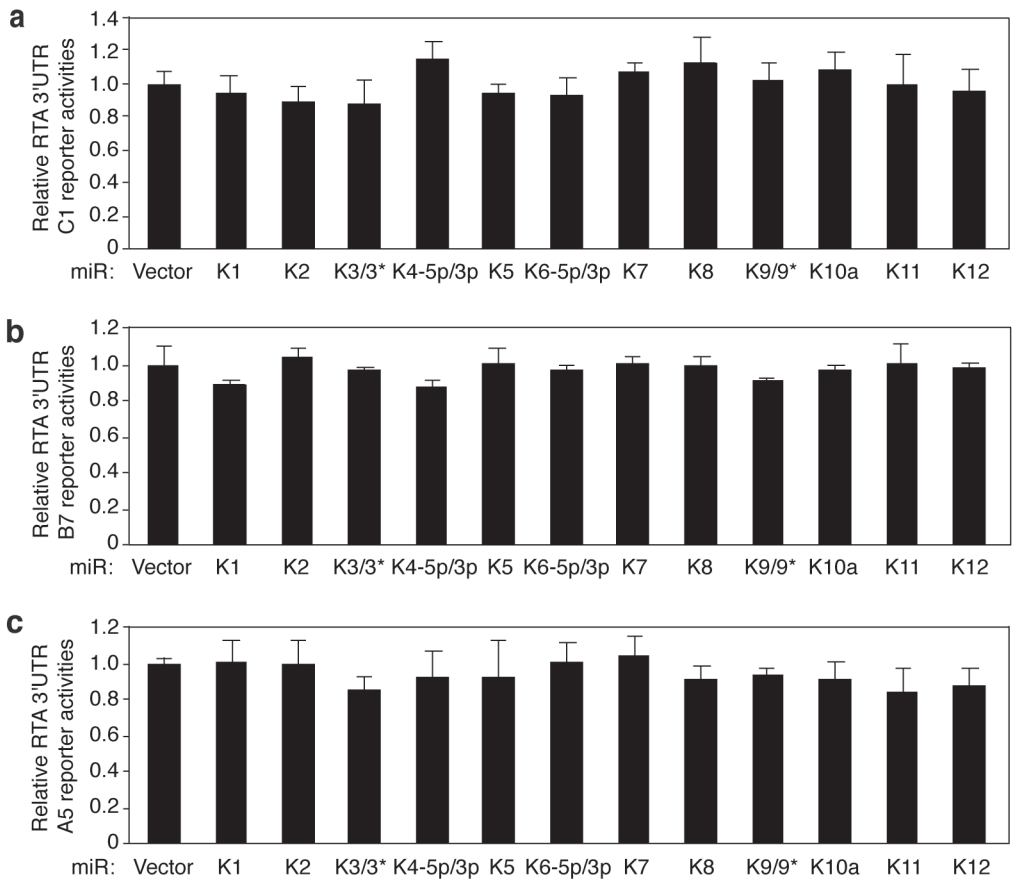

Figure S4 Effects of KSHV miRs on the 3'UTRs of RTA and ZTA transcripts measured in reporter assays in 293T cells. (**a-c**) Cells cotransfected with 3'UTR reporter constructs of RTA and ZTA type I transcript (**a**), type II transcript (**b**) and type III transcript (**c**), together with a β-galatosidase expression vector pSV-β-gal and a vector control or a expression vector of individual KSHV miRs were collected at 36 h post-transfection, and examined for luciferase activities, which were normalized to β-galatosidase activity. Data are means ± SEM from three (n = 3) independent experiments.

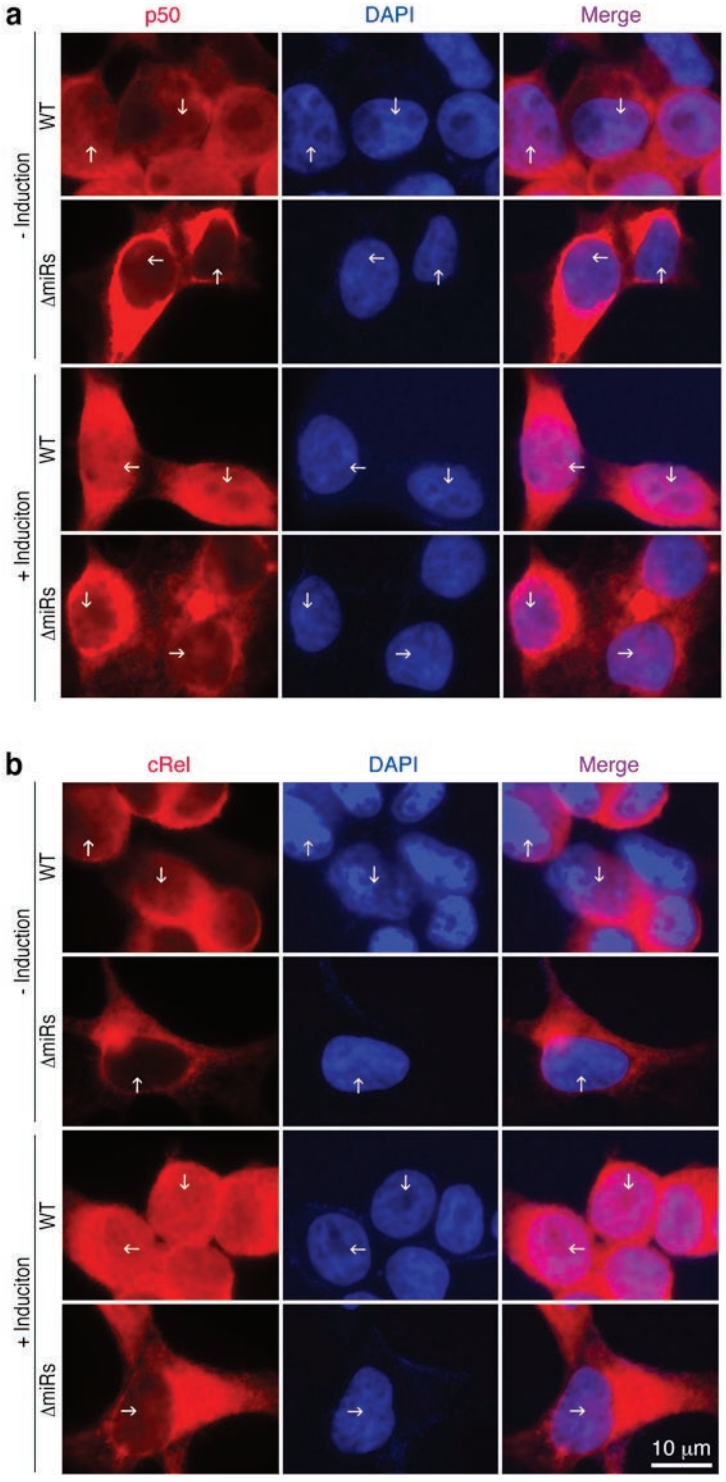

Figure S5 Immunofluorescence staining of NF-κB complex proteins p50 and cRel in WT and ΔmiRs 293T cells. (**a**) p50 staining in uninduced WT and ΔmiRs cells, and cells induced with TPA and sodium butyrate (T/B) for 24 h. (**b**) cRel staining in uninduced WT and ΔmiRs cells, and cells induced with T/B for 24 h. WT cells had stronger staining of p50 and cRel proteins in nuclei identified by DAPI than ΔmiRs cells had (white arrow).

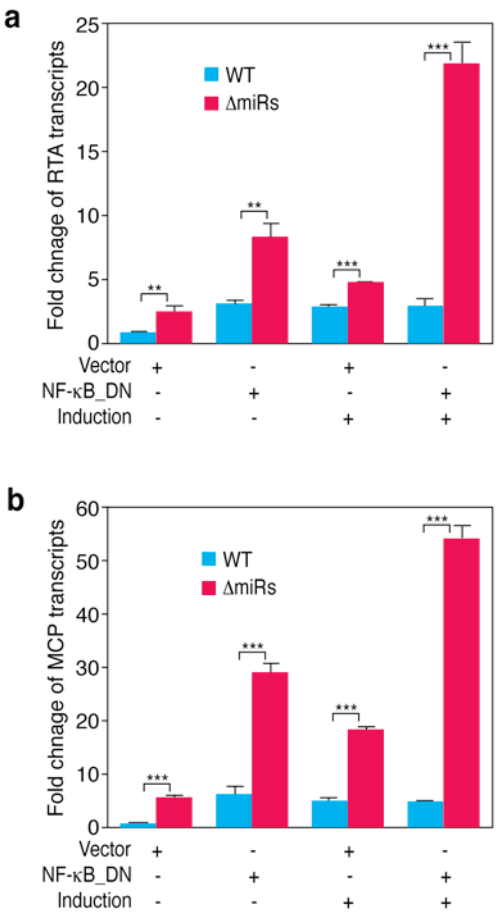

Figure S6 NF-κB pathway mediates the expression of KSHV lytic genes in 293T cells. (**a-b**) Levels of RTA (**a**) and MCP (**b**) transcripts examined by quantitative real-time reverse transcription PCR in WT and ΔmiRs cells transfected with the NF-κB dominant negative (DN) plasmid pIκB-αM or control vector for 72 h. Induced cells were treated with TPA and sodium butyrate for 48 h before collection. Data are means ± SEM from three (n = 3) independent experiments.

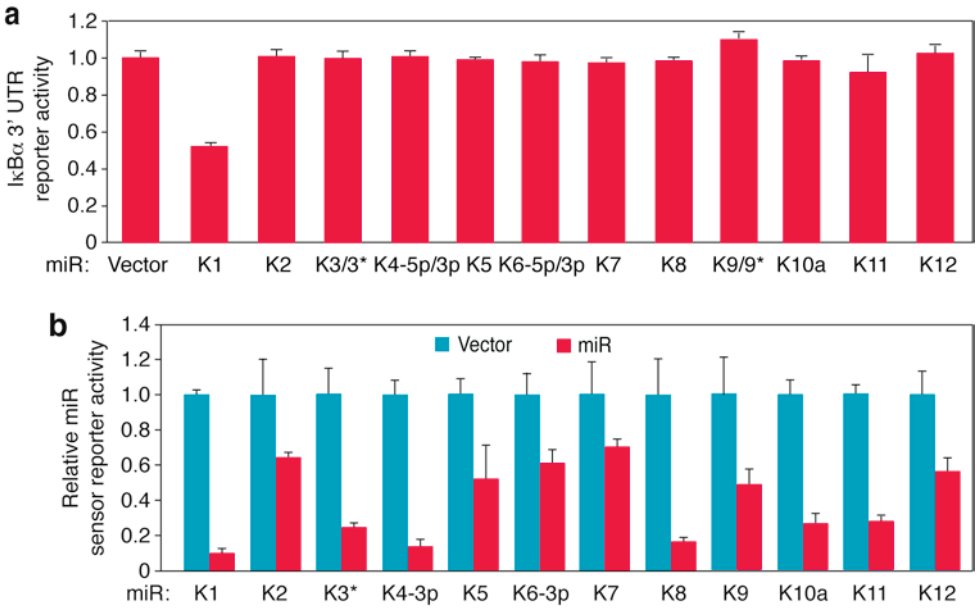

Figure S7 Identification of KSHV miR-K1 that suppresses IκBα 3'UTR reporter activity in 293T cells. (**a**) Relative IκBα 3'UTR reporter activities following cotransfection with individual miRs. Cells cotransfected with the IκBα 3'UTR reporter construct (IκBα-WT) together with a vector control or an expression vector of individual miRs were collected at 36 h post-transfection, and examined for luciferase activities. (**b**) Relative reporter activities of miR sensor reporters containing perfect matching sequences of their respective miRs following cotransfection with individual miRs. Cells cotransfected with the miR sensor reporters together with either a vector control or an expression vector of their respective miR were collected at 36 h post-transfection, and examined for luciferase activities. The expression constructs of KSHV miRs were functional as shown by their suppressive effects on the reporter activities of their respective sensor reporters. Data are means ± SEM from three (n = 3) independent experiments.

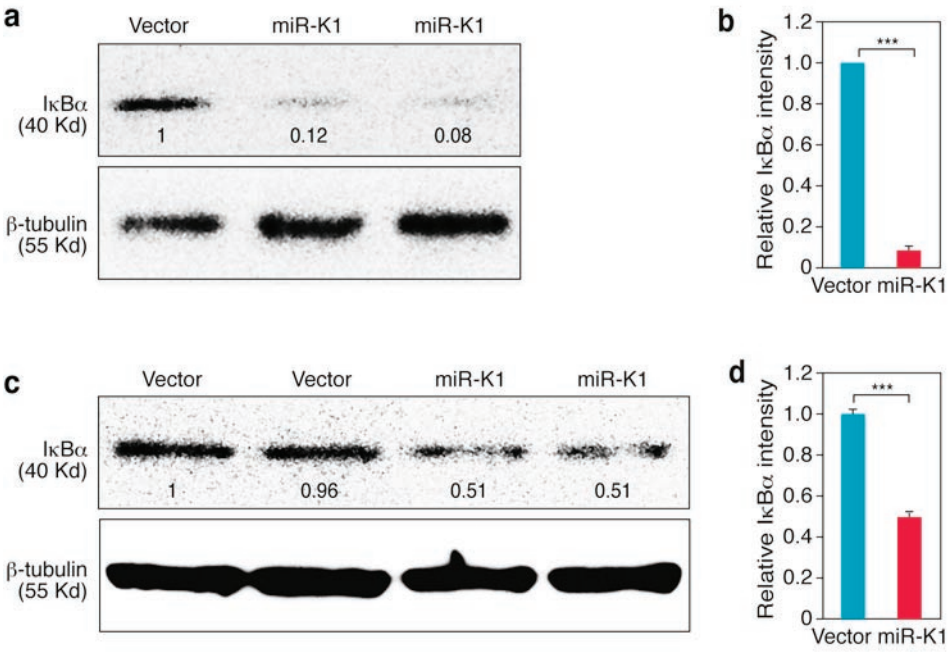

Figure S8 miR-K1 suppresses the expression of IκBα protein. Expression of miR-K1 suppressed IκBα protein in KSHV-negative (**a, b**) or ΔmiRs 293T cells (**c, d**). Cells transfected with a vector control or a miR-K1 expression vector were collected at 96 h post-transfection, and analyzed for IκBα protein by Western-blotting (**a, c**). Results are means of three images from three independent experiments (**b**, **d**).

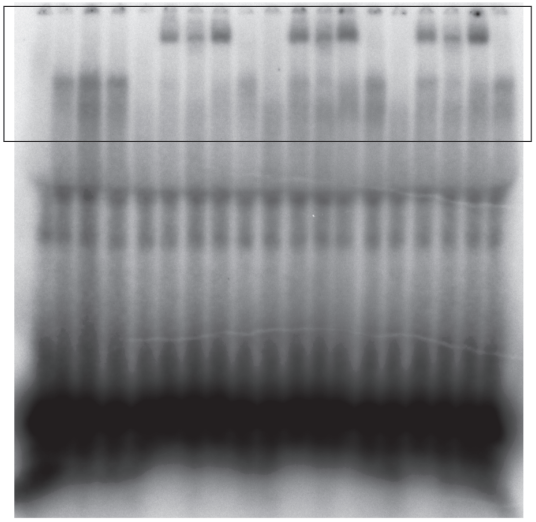

Fig. 2b: EMSA: NF-κB

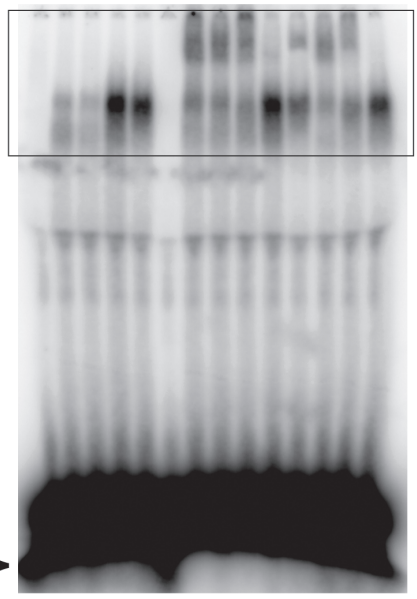

Fig. 2c: EMSA: NF-κB

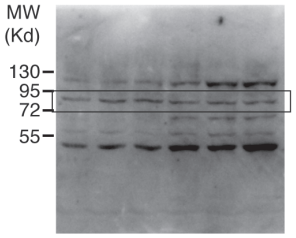

Fig. 3a, WB: IKKα

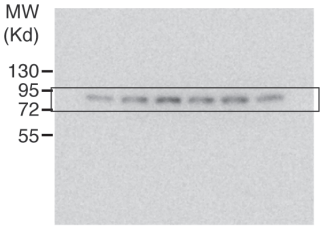

Fig. 3a, WB: IKKβ

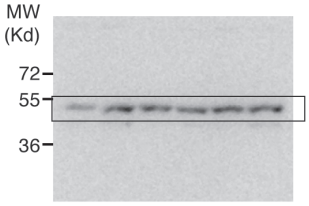

Fig. 3a, WB: IKKγ

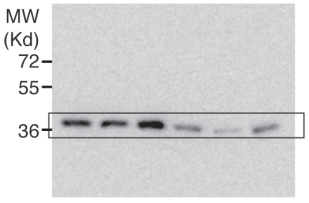

Fig. 3a, WB: IκBα

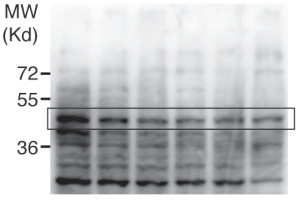

Fig. 3a, WB: IκBβ

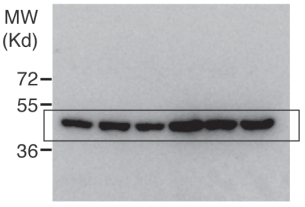

Fig. 3a, WB: IκBε

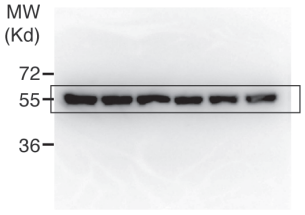

Fig. 3a, WB: β–tubulin

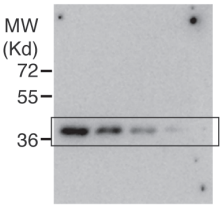

Fig. 3b, WB: IκBα

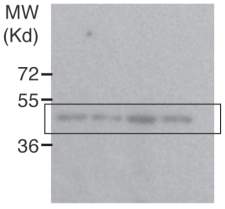

Fig. 3b, WB: IκBε

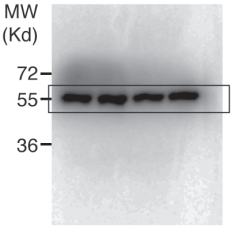

Fig. 3b, WB: β–tubulin

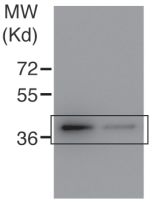

Fig. 3l, WB: IκBα

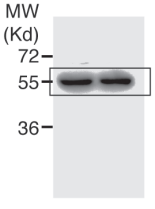

Fig. 3l, WB: β–tubulin

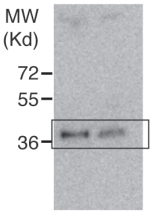

Fig. 3m, WB: IκBα

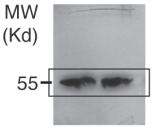

Fig. 3m, WB: β–tubulin

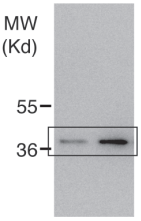

Fig. 4f, WB: IκBα

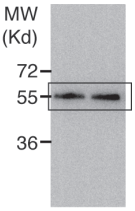

Fig. 4f, WB: β–tubulin

Figure S9 Full scans of key image data.

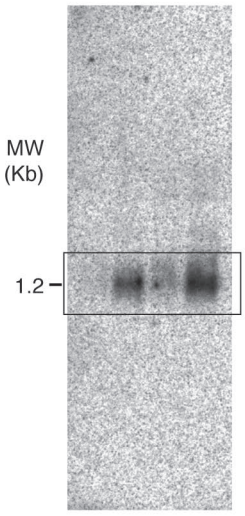

Fig. 4m, Northern:
Pan RNA

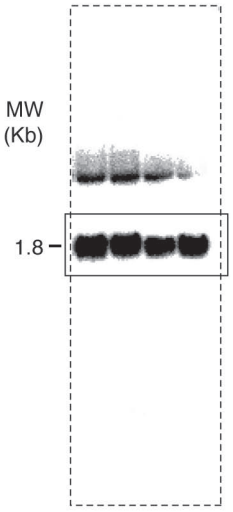

Fig. 4m, Northern:
β–actin

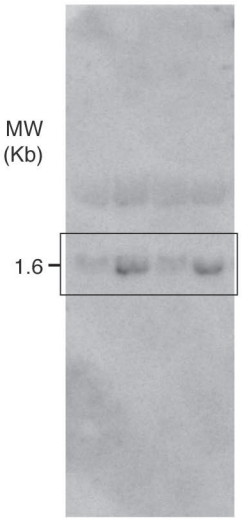

Fig. 4m, Northern:
ORF57

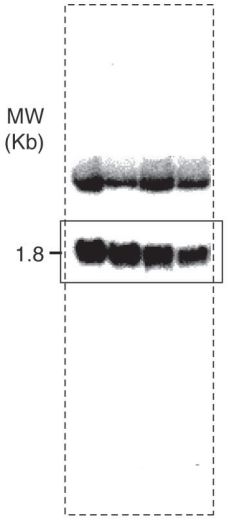

Fig. 4m, Northern:
β–actin

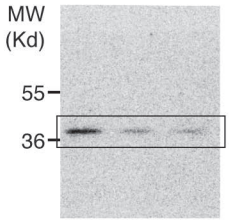

Fig. S11a, WB: IκBα

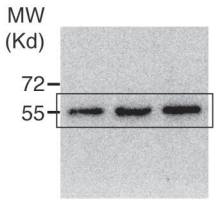

Fig. S11a, WB: β–tubulin

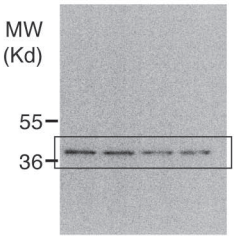

Fig. S11c, WB: IκBα

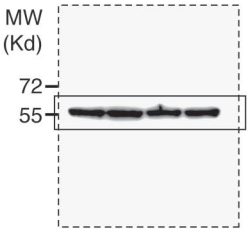

Fig. S11c, WB: β–tubulin

Figure S9 continued

Supplementary Table 1: Primers for reverse-transcription (RT) and PCR detection of KSHV genes and miRs

Target	Application	Primer
MCP	PCR	ORF25F: 5'-CTCGGCGACGTGCTATACAAT-3'
		ORF25R: 5'- TGCCGACAAGGACTGTACATG-3'
RTA	PCR	ORF50F: 5'-CACAAAAATGGCGCAAGATGA-3'
		ORF50R: 5'-TGGTAGAGTTGGGCCTTCAGTT-3'
vFLIP	PCR	ORF71F: 5'-GGATGCCCTAATGTCAATGC-3'
		ORF71R: 5'-GGCGATAGTGTTGGGAGTGT-3'
vCyclin	PCR	ORF72F: 5'-GCTGATAATAGAGGCGGGCAATGAG-3'
		ORF72R: 5'-GTTGGCGTGGCGAACAGAGGCAGTC-3'
LANA	PCR	ORF73F: 5'-GCAGACACTGAAACGCTGAA-3'
		ORF73R: 5'-AGGTGAGCCACCAGGACTTA-3'
GAPDH	PCR	GAPDH-F: 5'-CCCCTGGCCAAGGTCATCCA-3'
		GAPDH-R: 5'-ACAGCCTTGGCAGCGCCAGT-3'
Kshv-miR-K12-1	RT	Kshv-miR-K12-1 RT: 5'-GTCGTATCCAGTGCAGGGTCCGAGGTATTCGCACTGGATACGACGCTTAC-3'
Kshv-miR-K12-2	RT	Kshv-miR-K12-2 RT: 5'-GTCGTATCCAGTGCAGGGTCCGAGGTATTCGCACTGGATACGACCAGATC-3'
Kshv-miR-K12-3	RT	Kshv-miR-K12-3 RT: 5'-GTCGTATCCAGTGCAGGGTCCGAGGTATTCGCACTGGATACGACCGCTGC-3'
Kshv-miR-K12-4-5p	RT	Kshv-miR-K12-4 RT: 5'-GTCGTATCCAGTGCAGGGTCCGAGGTATTCGCACTGGATACGACCCTAGA-3'
Kshv-miR-K12-5	RT	Kshv-miR-K12-5 RT: 5'-GTCGTATCCAGTGCAGGGTCCGAGGTATTCGCACTGGATACGACCCGGCA-3'
Kshv-miR-K12-6-5p	RT	Kshv-miR-K12-6 RT: 5'-GTCGTATCCAGTGCAGGGTCCGAGGTATTCGCACTGGATACGACCCGATG-3'
Kshv-miR-K12-7	RT	Kshv-miR-K12-7 RT: 5'-GTCGTATCCAGTGCAGGGTCCGAGGTATTCGCACTGGATACGACAGCGCC-3'
Kshv-miR-K12-8	RT	Kshv-miR-K12-8 RT: 5'-GTCGTATCCAGTGCAGGGTCCGAGGTATTCGCACTGGATACGACCGTGCT-3'
Kshv-miR-K12-9	RT	Kshv-miR-K12-9 RT: 5'-GTCGTATCCAGTGCAGGGTCCGAGGTATTCGCACTGGATACGACAGCGGG-3'
Kshv-miR-K12-10a	RT	Kshv-miR-K12-10 RT: 5'-GTCGTATCCAGTGCAGGGTCCGAGGTATTCGCACTGGATACGACGCCACT-3'
Kshv-miR-K12-11	RT	Kshv-miR-K12-11 RT: 5'-GTCGTATCCAGTGCAGGGTCCGAGGTATTCGCACTGGATACGACTCGGAC-3'
Kshv-miR-K12-12	RT	Kshv-miR-K12-12 RT: 5'-GTCGTATCCAGTGCAGGGTCCGAGGTATTCGCACTGGATACGACCGGAGA-3'

Kshv-miR-K12-1	PCR	Kshv-miR-K12-1 F: 5’-CGCGCATTACAGGAAACTGGG-3’
Kshv-miR-K12-2	PCR	Kshv-miR-K12-2 F: 5’-CGTGCAACTGTAGTCCGGGTC-3’
Kshv-miR-K12-3	PCR	Kshv-miR-K12-3 F: 5’-CGCGCTCACATTCTGAGGACG-3’
Kshv-miR-K12-4-5p	PCR	Kshv-miR-K12-4 F: 5’-CGCGCAGCTAAACCGCAGTAC-3’
Kshv-miR-K12-5	PCR	Kshv-miR-K12-5 F: 5’-CGCGCTAGGATGCCTGGAACT-3’
Kshv-miR-K12-6-5p	PCR	Kshv-miR-K12-6 F: 5’-cgcgcCCAGCAGCACCTAATC-3’
Kshv-miR-K12-7	PCR	Kshv-miR-K12-7 F: 5’CGCGCTGATCCCATGTTGCTGGC-3’
Kshv-miR-K12-8	PCR	Kshv-miR-K12-8 F: 5’-CGCGCTAGGCGCGACTGAGAG-3’
Kshv-miR-K12-9	PCR	Kshv-miR-K12-9 F: 5’-CGCGCACCCAGCTGCGTAAAC-3’
Kshv-miR-K12-10a	PCR	Kshv-miR-K12-10 F: 5’-CGTGCTAGTGTTGTCCCCCCG-3’
Kshv-miR-K12-11	PCR	Kshv-miR-K12-11 F: 5’-CGCGCTTAATGCTTAGCCTGT-3’
Kshv-miR-K12-12	PCR	Kshv-miR-K12-12 F: 5’-CGCGCACCAGGCCACCATTCC-3’
All KSHV miRs	PCR	Kshv-miR-K12 R: 5’-GTGCAGGGTCCGAGGT-3’